Biosensors and Bioelectronics 54 (2014) 492–498

Contents lists available at ScienceDirect

Biosensors and Bioelectronics

journal homepage: www.elsevier.com/locate/bios

Testing synthetic amyloid-β aggregation inhibitor using single molecule atomic force spectroscopy

Francis T. Hane [a], Brenda Y. Lee [a], Anahit Petoyan [b], Arvi Rauk [b], Zoya Leonenko [a,c,*]

[a] University of Waterloo, Department of Biology, 200 University Ave. West, Waterloo, Ontario, Canada N2L 3G1
[b] University of Calgary, Department of Chemistry, 2500 University Drive NW, Calgary, Alberta, Canada T2N 1N4
[c] University of Waterloo, Department of Physics and Astronomy, 200 University Ave. West, Waterloo, Ontario, Canada N2L 3G1

ARTICLE INFO

Article history:
Received 25 July 2013
Received in revised form
13 October 2013
Accepted 29 October 2013
Available online 11 November 2013

Keywords:
Single molecule force spectroscopy
Amyloid-β aggregation
Fibril formation
Aggregation inhibitor
Molecular dynamics simulations
Alzheimer's disease

ABSTRACT

Alzheimer's disease is a neurodegenerative disease with no known cure and few effective treatment options. The principal neurotoxic agent is an oligomeric form of the amyloid-β peptide and one of the treatment options currently being studied is the inhibition of amyloid aggregation. In this work, we test a novel pseudopeptidic aggregation inhibitor designated as SG1. SG1 has been designed to bind at the amyloid-β self-recognition site and prevent amyloid-β from misfolding into β sheet. We used atomic force spectroscopy, a nanoscale measurement technique, to quantify the binding forces between two single amyloid peptide molecules. For the first time, we demonstrate that single molecule atomic force spectroscopy can be used to assess the effectiveness of amyloid aggregation inhibitors by measuring the experimental yield of binding and can potentially be used as a screening technique for quick testing of efficacy of inhibitor drugs for amyloid aggregation.

© 2013 Elsevier B.V. All rights reserved.

1. Introduction

Alzheimer's disease (AD) is a neurodegenerative disease associated with progressive memory loss and dementia. Current research supports the hypothesis that Alzheimer's is caused by the misfolding of the amyloid-β (Aβ) peptide into β sheets which then aggregate into toxic oligomers (Chiti and Dobson, 2009) and fibrils. AD is a complex disease associated with a number of potential factors including aging (Bertram and Tanzi, 2005), genetics (Bertram and Tanzi, 2005), metals dyshomeostasis (Bush and Tanzi, 2008), protein–lipid interactions (DiPaolo and Kim, 2011), vascular disorders (Roy and Rauk, 2005), and loss of acetylcholine receptors (Whitehouse et al., 1986). Pharmaceutical therapies have focused on attacking underlying factors associated with Alzheimer's (Robertson and Mucke, 2006). For example, γ-secretase inhibitors have been developed in an attempt to stop the cleaving of amyloid-β from its precursor protein, the amyloid precursor protein (APP) (Citron, 2004). Despite extensive research and funding, no therapy has yet been shown to reverse the symptoms associated with Alzheimer's in human trials, and even the most efficacious therapies are not curative, but only delay the onset of symptoms (Neugroschl and Sano, 2010).

Aβ begins its pathological aggregation by misfolding into an internal β sheet between the amino acids 17–23 and 28–35. The amino acids (24–27) form a β-hairpin to allow the peptide to fold back on itself (Petkova et al., 2002; Sciarretta et al., 2005). After misfolding into a hairpin, the peptide may bind to another Aβ peptide, acting as a nucleus for further peptide aggregation. The self-recognition site (17–23) (Tjernberg et al., 1996, 1997) is responsible for the aggregation of Aβ into dimers and higher oligomers. Blocking this site effectively prevents the misfolding and subsequent aggregation. In the absence of sufficient peptide clearance, this aggregation leads to the formation of toxic amyloid aggregates (Harper and Lansbury, 1997).

The Aβ sequence (13–23), which incorporates the self-recognition site, has been a target for amyloid aggregation inhibitors (Mothana et al., 2009) which are designed to have a high affinity for the self-recognition site and "block" the peptide from self-dimerization. Rauk and co-workers developed a series of pseudopeptidic novel amyloid inhibitors that bind to and act on this self-recognition site (Mothana et al., 2009; Roy, 2010). These inhibitors consist of a series of modified amino acids including methylated amino acids. A structure of SG1 is show in Fig. 2b. These inhibitors were synthesized and tested using a combination of circular dichroism and thioflavin T fluorescence assay to look for evidence of peptide aggregation. These methods have a

* Corresponding author at: University of Waterloo, Department of Physics and Astronomy, 200 University Ave. West, Waterloo, Ontario, Canada N2L 3G1.
Tel.: +1 519 888 4567x38273; fax: +1 519 746 8115.
E-mail address: zleonenk@uwaterloo.ca (Z. Leonenko).

0956-5663/$ - see front matter © 2013 Elsevier B.V. All rights reserved.
http://dx.doi.org/10.1016/j.bios.2013.10.060

characteristically low throughput because a period of 24 h or more is needed for the peptide to aggregate into a recognizable form to determine the effect of the inhibitor on the aggregation properties. Atomic force spectroscopy (AFS) is a nanoscale technique based on atomic force microscopy (AFM) and is often used to probe interactions between two single molecules. We used this technique to test the efficacy synthetic amyloid inhibitor SG1 and demonstrated that SG1 reduces the number of binding events between two Aβ peptides by as much as 81%. In addition, we used atomic force microscopy and molecular dynamics simulations for comparison with AFS data and demonstrated with all these methods that the aggregation of Aβ is greatly reduced in the presence of SG1.

2. Material and methods

To follow the effect of SG1 on Aβ aggregation and fibril formation, AFM was used in both imaging mode and force spectroscopy mode. In imaging mode a sharp scanning probe (AFM tip) scans the sample surface and the forces of interaction at each point are measured to produce an image of surface morphology (Binnig et al., 1986), which allows for high resolution imaging and visualization of the formation of Aβ oligomers and fibrils. To measure single molecule binding forces between peptides, AFM was used in force spectroscopy mode, in which the AFM probe, with an Aβ peptide attached to it was moved repeatedly towards and away from the mica surface, also bound with peptides, and the interaction force was measured as a function of probe-sample separation at pN resolution. For these experiments attachment of the Aβ peptide to both AFM probe and the surface is required. Except as noted, we used chemical modification protocols as previously described (Hane et al., 2013). The details of experimental procedures are outlined below.

2.1. Tip and mica modification for force spectroscopy.

A Bruker MSNL Silicon Nitride AFM cantilever was cleaned in ethanol, washed with MilliQ water and dried in a gentle stream of nitrogen. The cantilever was then placed under UV light for 30 min. Freshly cleaved mica slides and cantilevers were modified with 1-(3-aminopropyl) silatrane (APS), incubated in a 167 μM solution of 35 nm *N*-hydroxysuccinimide-polyethylene glycol-maleimide (NHS-PEG-mal) (Laysan Bio (Arab, AL)) for 3 h, rinsed with DMSO, and then dried with a gentle stream of nitrogen.

2.2. Amyloid-β (1–42) preparation and surface binding force spectroscopy measurements

Cys-Amyloid-β (1–42) was purchased from Anaspec (Fremont, CA) and dissolved in DMSO at a concentration of 1 mg/mL. The Aβ stock solution was diluted in HEPES buffer (50 mM, pH 7.4, NaCl ionic strength 150 mM) to a final concentration of 20 nM. *Tris*(2-carboxyethyl)phosphine (TCEP, 200 nM) was added to the dilute Aβ solution in equal volume. The Aβ was stored for 15 min, and then centrifuged at 14,000 RPM for 15 min (Kim et al., 2011). Mica and cantilevers were immersed in the Aβ solution for 30 min, rinsed with HEPES buffer, treated for 10 min with β-mercapto-ethanol. Both cantilever and mica were rinsed with HEPES buffer, and stored in HEPES buffer until use.

2.3. Preparation of SG1 inhibitor solution

SG1 was synthesized using fmoc-chemistry method (Roy, 2010). SG1 was lyophilized and stored in powdered form in −20 °C. When ready for experimental use, SG1 was dissolved in HEPES buffer (50 mM, 150 mM NaCl, pH 7.4). A 2 μM stock solution was prepared using serial dilutions. From the stock solution, final aliquots of 20 nM, 40 nM and 200 nM were prepared for experimental force spectroscopy experiments.

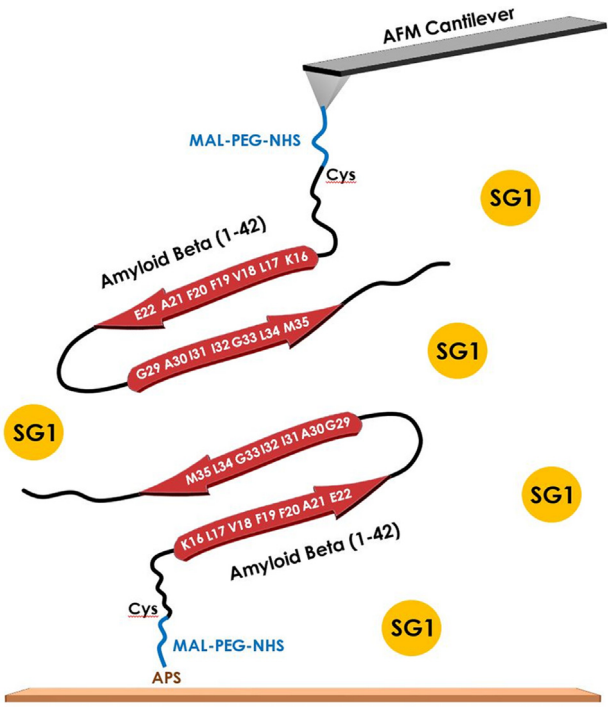

Fig. 1. Schematic of force spectroscopy experiment. A schematic of the experimental setup of force spectroscopy experiments, showing Aβ bound to the substrate and AFM tip via the PEG linker with aggregation inhibitor SG1 in the aqueous solution. A silanated surface is modified with NHS-PEG-maleimide. A cysteine residue is bound to the N-terminus of Aβ peptide to act as a binding site for the maleimide group of the linker molecule.

2.4. Atomic force spectroscopy

A JPK Nanowizard II atomic force microscope (AFM) was used for force measurements in contact mode, where deflection of cantilever versus distance was recorded. The mica substrate with attached Aβ peptide was placed on the stage and the liquid cell was filled with HEPES buffer. An AFM probe with Aβ attached was brought into contact with the substrate (approach) to allow the peptides attached to the probe to bind to peptides attached to substrate (Fig. 1) and then the probe was retracted from the substrate to force the unbinding of the two peptides. A series of force curves were taken with an approach and retract velocity of 400 nm/s. The ratio of observed events to the total number of approaches is referred to as the experimental yield. The yields from separate experiments varied from 3% to 30%. At least 900 force plots were captured in each experiment. More than 10,000 approaches were made and force plots collected to achieve a statistically valid number of rupture events. Nine hundred approaches were done for each experiment (i.e. 900 approaches for Aβ only, 900 approaches with 20 nM SG1, 900 approaches with 40 nM SG1, 900 approaches 200 nM SG1). Each experiment was repeated 3 times. We used Bruker MLCT cantilevers with spring constants between 100 and 700 mN/m, calibrated using JPK software via the thermal noise method (Hutter and Bechhoefer, 1993). In our experiments, we prepared a set of chemically modified cantilevers and substrates in advance, and once the inhibitor solution is ready, the cantilever can be loaded into the AFM and a control experiment can be completed consisting of ~1000 approaches. The inhibitor solution can then be added to the liquid

cell and another ~1000 approaches conducted. This can be conducted within 30–40 min.

2.5. Force curve analysis

All force curves collected were reviewed for unbinding events. An unbinding event is indicated by at least one adhesion peak (typical force plot is shown in Fig. 3a). Force curves demonstrating no unbinding event were discarded. The force curves contained unbinding events were analyzed using JPK SPM Data Processing (v 4.2.50). A Gaussian fit was applied to determine the most probable unbinding force using OriginPro 8.6 software. We determined the percent yield by dividing the force curves with unbinding events by the total number of curves collected.

2.6. AFM imaging of amyloid-β and SG1 incubated in solution.

Aβ (1–42) was purchased in lyophilized powder from rPeptide (Bogart, GA), pretreated according to the Fezoui procedure (Fezoui et al., 2000) to ensure monomeric form. The Aβ was dissolved in HEPES buffer (20 mM HEPES and 100 mM NaCl, pH 7.4) and was immediately used to prepare the sample solutions at a final concentration of 110 μM Aβ (1–42). The inhibitor SG1 was added at a 1:1 molecular ratio of SG1 to Aβ. The control solution had no inhibitor added. Solutions were incubated at 1, 6, and 24 h at room temperature. After each incubation period, 100 μL of each solution was deposited onto freshly cleaved mica slides and incubated at room temperature for 5 min. Mica slides were then rinsed 5 times with 50 μL aliquots of distilled H_2O, dried for 2 min with a gentle stream of nitrogen gas and imaged in air in intermittent contact mode using JPK Nanowizard II AFM. We used silicon AFM probes (VISTA), with a spring constant of 40 N/m, resonance frequency of 300 kHz, and an aluminum reflex coating. Multiple 50 × 50 μm images and 5 × 5 μm images were collected from each sample at a resolution of 2048 pixels and used for statistical analysis. AFM images were analyzed to extract the size of oligomers, fibrils and oligomer to fibril ratios using JPK image processing software and ImageJ v. 1.43 u software.

2.7. Molecular dynamics simulations

The initial structures of SG1, Aβ (13–23), Aβ (13–23)–Aβ (13–23), and SG1–Aβ (13–23) were obtained as described

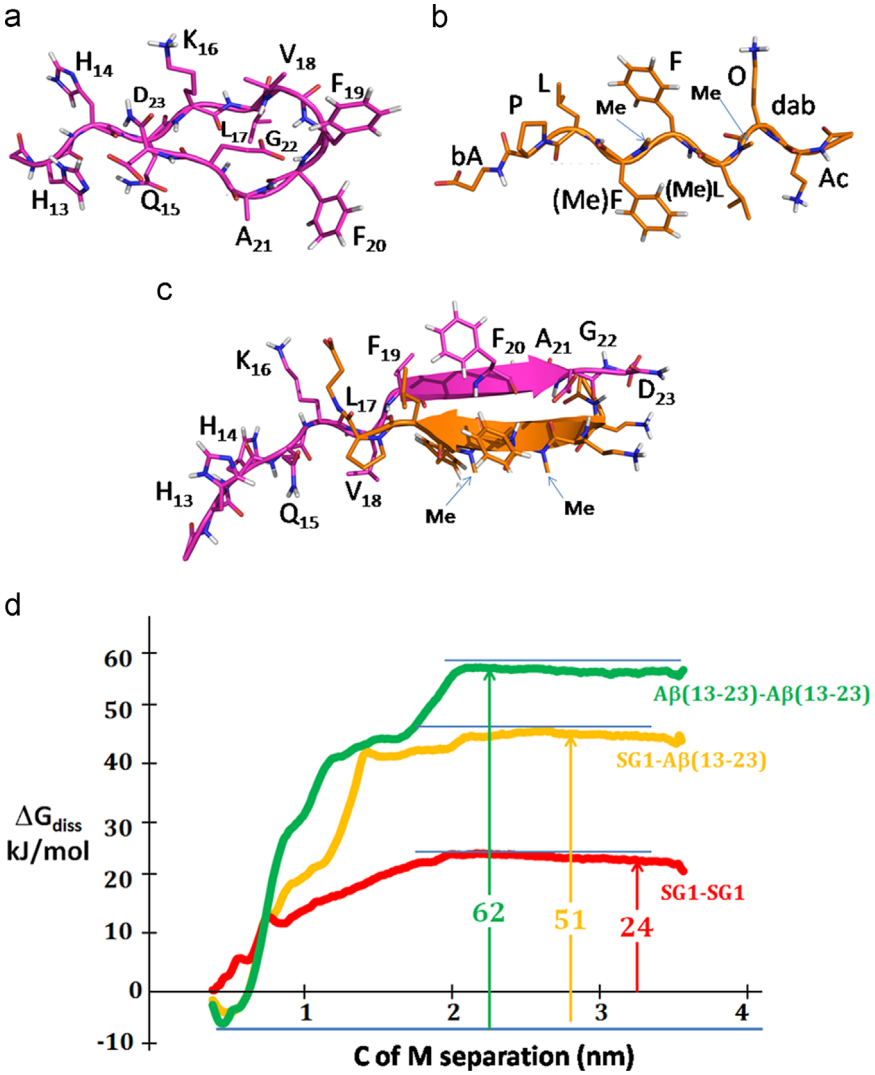

Fig. 2. Molecular dynamics simulations showing mechanism of action of SG1: (a) the structure of Aβ (13–23) in its most stable conformation. (b) The structure of SG1 in its most stable conformation (β-strand): SG1=Ac-dab-O-(Me)L-F-(Me)F-LP-bA-COOH where dab=diaminobutyric acid, O=ornithine, (Me)L=*N*-methylleucine, (Me)F=methylphenylalanine, and bA=β-alanine; (c) The structure of the complex of SG1 (gold) and Aβ (13–23) (magenta). The complex is predominantly an antiparallel β sheet. (d) Free energies of dissociation (ΔG_{diss}) in kJ/mol, of Aβ(13–23)-Aβ(13–23), SG1–Aβ(13–23) and SG1–SG1. All form antiparallel dimeric complexes. (For interpretation of the references to color in this figure caption, the reader is referred to the web version of this article.)

earlier (Mothana et al., 2009). The monomeric Aβ receptor model, Aβ(13–23), was acetylated at the N-terminus, residue 13 (His13) and N-methylated at residue 23 (Asp23). The SG1–SG1 dimer was determined as described previously (Mothana et al., 2009). All MD simulations were performed using the Gromacs 4.5 suite of software (Hess et al., 2008; Van der Spoel

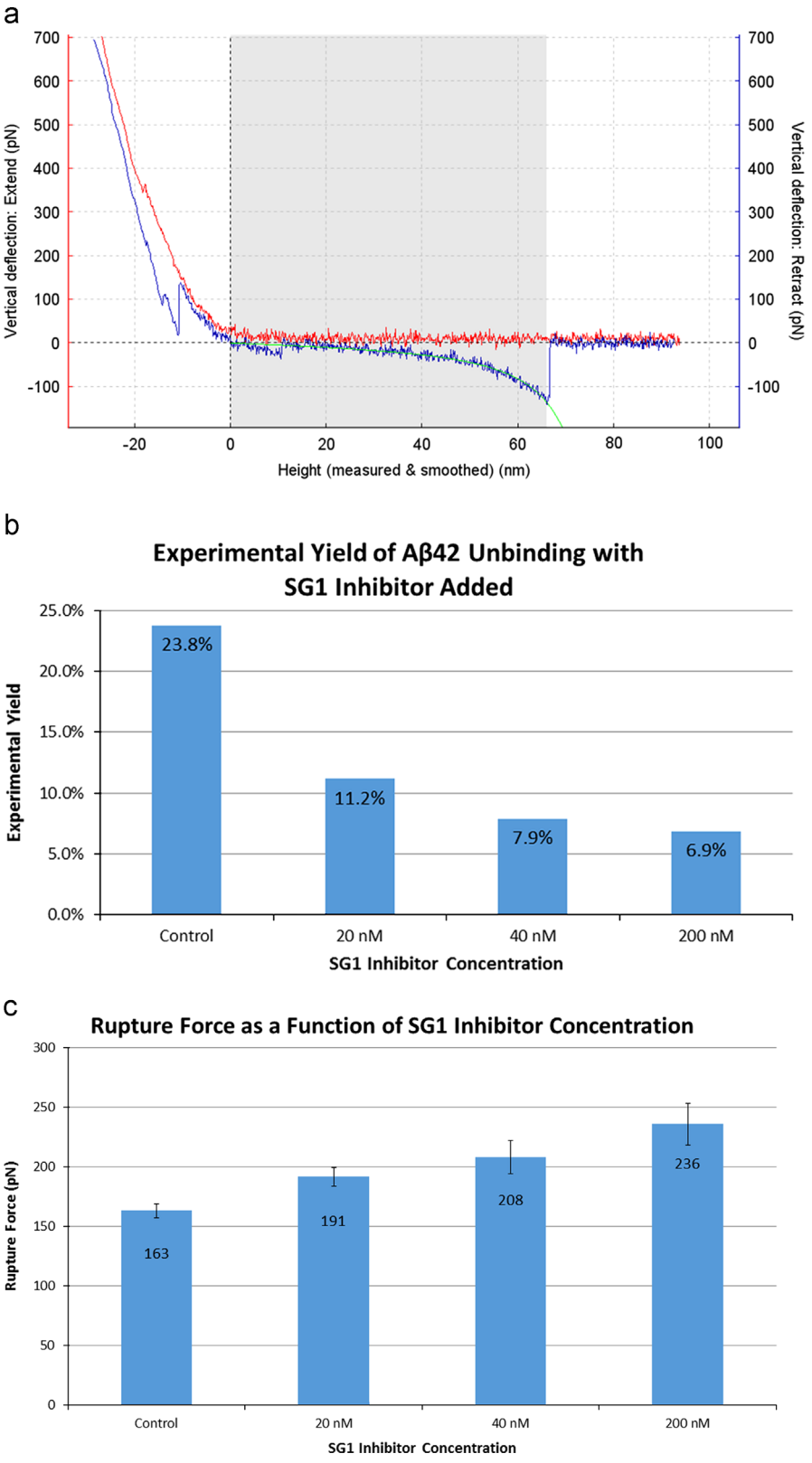

Fig. 3. (a) Typical unbinding force curve. The tip approaches the surface (red) until the AFM senses a repulsive force resulting from the tip interacting with the sample. The tip is then retracted (blue). As the tip is retracted, an interaction between the two molecules is measured until there is a sudden rupture at which point the cantilever returns to its original unbent position. If a binding event occurs, the retraction plot shows adhesion peak; (b) Dependence of experimental yield of binding on concentration of SG1 inhibitor; (c) Rupture force dependence on inhibitor concentration. (For interpretation of the references to color in this figure caption, the reader is referred to the web version of this article.)

et al., 2005; Lindahl et al., 2001; Berendsen et al., 1995). Previously, the free energy perturbation technique called "Atomic Force Microscopy" or AFM was used to calculate the free energy of binding of different complexes (Mothana et al., 2009). The binding results presented in this work were reevaluated with the more accurate technique, "Umbrella Sampling," in which selected frames along the AFM potential curves are re-equilibrated and re-assembled into complete potential curves by the "Weighted Histogram Analysis Method" (WHAM). Each dimer had 30 windows and each window was equilibrated for 20 ns with force constant 1000 kJ/ (mol nm^2) at physiological pH (7.4) and temperature (310 K).

3. Results

A schematic of the experimental set up is shown in Fig. 1 with one Aβ peptide bound to the tip and another to substrate via intermediate PEG linkers.

Amyloid aggregation inhibitor SG1 binds to the Aβ self-recognition site (17–23), preventing the dimerization and further aggregation of Aβ. By binding to this site, the inhibitor physically prevents the two structured sections from coming into contact and forming the prerequisite hairpin. In Fig. 2a, the structure of most stable conformation of Aβ (13–23) is shown, which is folded conformation, stabilized by intramolecular H-bonds between Glu22 and the amido N–H of residues Val18–A21. The most stable

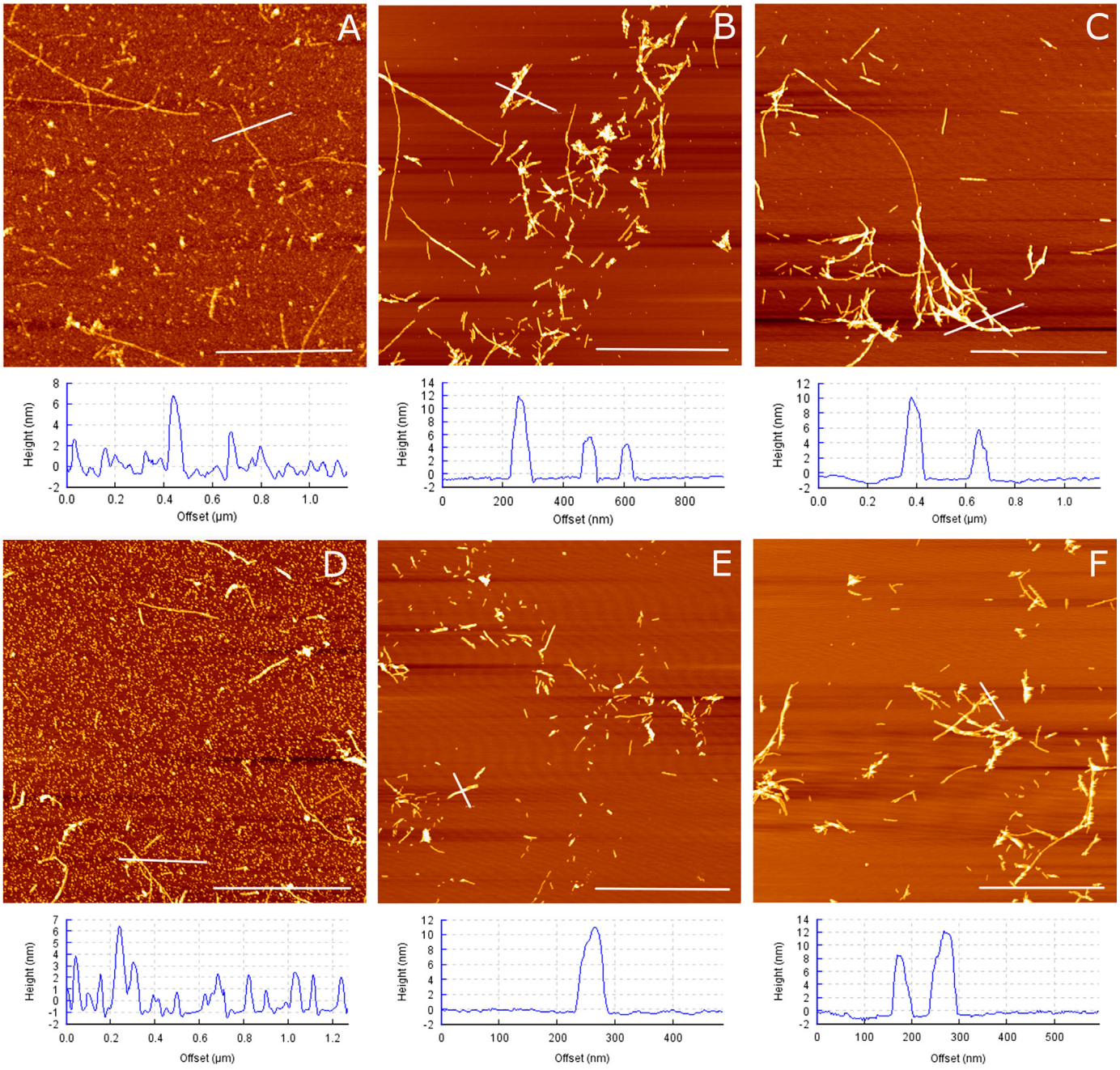

Fig. 4. AFM images of Amyloid Fibril formation with and without Inhibitor. Aβ only (A, B, C) and Aβ with inhibitor SG1 incubated for 1, 6 and 24 h, respectively (D, E, F). SG1 and Aβ concentrations were identical at 110 μM. After incubation for 1, 6, and 24 h (images from left to right) at room temperature, 100 μL aliquots of each solution were deposited on freshly cleaved mica for 5 min, washed, dried and imaged in air. Below each image a cross-section is shown, indicating the height of the aggregates. The scale bar is equal to 1 μm.

conformation of SG1 is a β-strand (Fig. 2b). SG1 is designed to make an antiparallel β sheet with the self-recognition site, Aβ (17–23). The structure of the SG1 peptide shown in Fig. 2a was obtained by MD simulations and the binding between SG1 and Aβ (13–23) fragment responsible for β-sheet formation was calculated. When SG1 binds to Aβ, N-methylation at one edge of the β strand ensures that SG1 cannot propagate a β sheet from that edge Fig. 2c shows the complex formed as a result of binding between SG1 and Aβ (13–23), which is predominantly an antiparallel β-sheet.

Fig. 2d shows free energy curves for the dissociation of the Aβ (13–23) dimer, the SG1/Aβ (13–23) complex and the SG1 dimer obtained from MD simulations. The free energies of dissociation are 62, 56, and 40 kJ/mol, respectively.

Using AFS we measured unbinding forces and observed a noticeable reduction in the experimental yield in the presence of SG1 (from 24% in control experiment to 11.2% with equimolar concentrations SG1). Higher inhibitor concentrations of 40 nM and 200 nM resulted in experimental yields of 7.9% and 6.9%, respectively.

A typical force curve is shown in Fig. 3a, with adhesion peak in the withdraw part of the force plot (blue). The unbinding event starts at a ~65 nm which correlates with the length of two PEG linkers (each ~35 nm). MD data as shown in Fig. 2b do not include a PEG linker and separation is therefore considerably less.

Fig. 3b and c displays the results of a typical experiment with mean rupture force shown (Fig. 3c) and the experimental yield of this experiment (Fig. 3b). While a significant reduction in the experimental yield was observed as a function of inhibitor concentration (Fig. 3b), a quasi-linear increase in the unbinding force was also observed at higher concentrations of SG1 (Fig. 3c).

The effectiveness of the inhibitor was also validated by atomic force microscopy imaging. SG1 was added into the Aβ solution and after incubation for 1, 6 and 24 h, the aggregates that were formed in solution were deposited on mica and imaged by AFM (Fig. 4) in air. In the absence of inhibitor, typical amyloid fibrils grew in width and length as a function of incubation time. When the aggregation inhibitor SG1 was added, a reduction in the number of fibrils was observed especially at earlier incubation times of 1 and 6 h. We define the oligomer qualitatively as any of small globular structures not resembling a long fibrillar form. Other authors have referred to these structures as Aβ derived diffusible ligands (ADDL) (Lambert et al., 1998), or prefibrillar oligomers (Glabe, 2008). Fibrils formed with inhibitor present were considerably smaller in length and width than the fibrils observed in the control samples. A statistical analysis of height distribution for Aβ control shows that the mean aggregate heights for 1, 6, and 24 h were very similar: 6.47, 7.00, and 6.39 nm, respectively. For samples with SG1, the mean aggregate heights were changing with time: 3.13, 5.17, and 7.87 nm for 1, 6 and 24 h, respectively.

The size of fibrils increased as a function of time for control samples. When SG1 inhibitor was added, fibril growth was considerably slower, and fibrils produced were shorter. The mean fibril lengths for amyloid-β were 262, 571, 715 nm at 1, 6 and 24 h, respectively. For the SG1 sample, we calculated mean fibril length of 83, 193, and 301 nm at 1, 6, 24 h, respectively. We analyzed the images to deduce oligomer to fibril ratio (Fig. 5). After 1 h of incubation, both the control sample and the SG1 sample showed twice as much oligomers compared to fibrils. As incubation time increased, the control sample showed a large increase in the fibril/oligomer ratio to 10.3 indicating that there were 10 times as many monomers in fibrillar form than the oligomeric form. At 24 h of incubation, the fibril to oligomer ratio increased to 12.5. With the SG1 present, the fibril to oligomer ratio was much lower: 0.5 at 1 h and increased to only 9.7 after 24 h of incubation (Fig. 5).

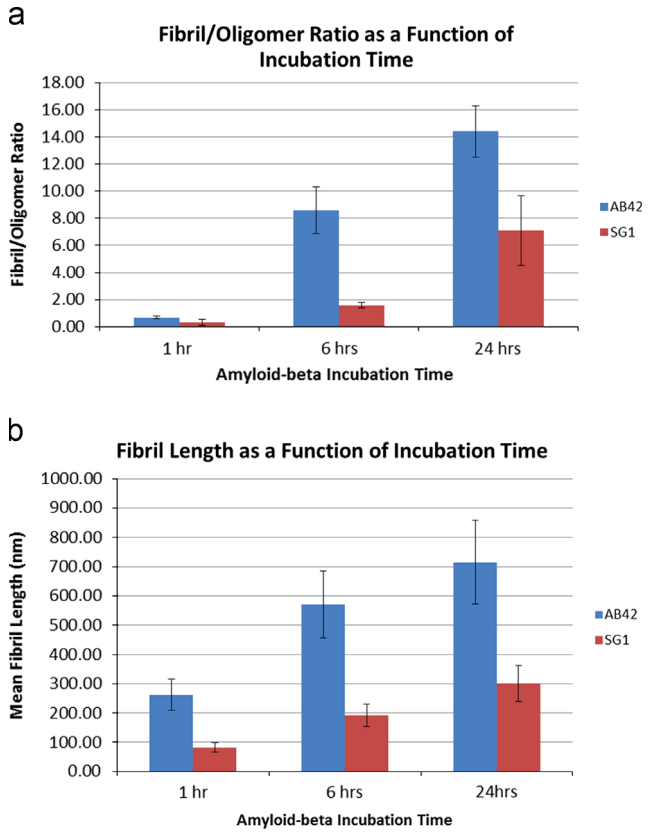

Fig. 5. Statistical analysis of AM images. (a) Fibril to oligomer ratio and (b) Fibril length as a function of incubation time and presence of inhibitor.

4. Discussion

The goal of this study was to demonstrate that amyloid aggregation inhibitor SG1 can be used to slow the aggregation of the Aβ peptide. In addition, we wanted to show the potential of using AFS for quick testing of inhibitor drugs for amyloid fibril formation before they go to cellular, animal studies or clinical trials.

The first step in any aggregation process is the formation of a critical nucleus which begins with the dimerization of two molecules. If this initial process can be inhibited, aggregation will not occur, or at least the lag time associated with aggregation will increase or the aggregation rate will be lowered to allow for physiological clearance mechanisms to clear aggregates before they accumulate and become neurotoxic.

In past AFS experiments, the unbinding force itself has been used to characterize binding of molecules (Hinterdorfer and Dufrêne, 2006). In this work we show that the most useful parameter for testing inhibitors is the experimental yield of binding/unbinding events. Our objective was to determine a binary process: “binding” or “no-binding” event. We demonstrate that the greatest reduction in amyloid dimerization occurs when a small concentration (20 nM) of SG1 inhibitor is present in the solution. As the concentration of inhibitor increases, the experimental yield decreases in an inverse exponential manner (Fig. 3b). In correlation with experiments, the MD data demonstrate that SG1 binds to Aβ (13–23) fragment, a self-recognition part of Aβ (1–42), a slightly less strongly than Aβ binds to itself, but significantly stronger than SG1 binds to itself. The N-methylation pattern of SG1 ensures that when it binds at the self-recognition site of Aβ, it prevents the amino acid domains (16–22) and (29–35) from binding with one another- the initiating event of the aggregation

cascade. An ideal inhibitor will result in no Aβ dimerization (no-binding), but there is a limit to the inhibitor concentration able to bind to a very sparse coverage of surface bound peptides. The reason there are still amyloid-amyloid binding events in the inhibitor environment is because the inhibitor has not bound all available Aβ peptide. As the inhibitor concentration increases, the probability of an inhibitor molecule coming into contact with a surface or tip bound Aβ peptide increases. The difference between 40 nM and 200 nM concentrations of inhibitor is only 1% experimental yield making the inhibitor concentration dependence appear asymptotic. The AFM images in Fig. 4 show that some aggregation is still observed even with inhibitors present. Furthermore, we noticed that higher inhibitor concentrations resulted in an increase of unbinding force. From MD simulations we conclude that SG1 induces a conformational change in Aβ, converting the self-recognition region into a β strand. This conformational change costs energy, making the calculated binding affinity less than the actual interaction between two β strands. Once the energy cost has been paid, further interaction may appear to be stronger. This may cause the increase of the unbinding forces that we observe experimentally with the increase of concentration of SG1.

The analysis of AFM images indicates that the structure of the oligomers that were different when SG1 was present. Without the inhibitor, Aβ forms characteristic oligomers of β-sheet structure which grow in length to form long fibrils. When the inhibitor was present, characteristic Aβ–Aβ arrangement was disturbed, which resulted in the observation of different heights of oligomers and less fibril growth (Figs. 4 and 5). Extensive evidence suggests that the dimerization and further nucleation of an amyloid oligomer is the rate limiting step in the fibrillization process (Stefani, 2012). Our AFM data indicates that SG1 may not slow the nucleation of Aβ but rather inhibit the polymerization of oligomers into amyloid fibrils with β-sheet structure. Thus, all three factors, the change in the unbinding force, the reduction of experimental yield of binding, and the decrease of fibril formation indicate that the SG1 inhibitor successfully suppresses the typical pathway of Aβ–Aβ interaction, which results in characteristic (Aβ–Aβ) unbinding forces and formation of fibrils and oligomers with β-sheet structure.

Alzheimer's disease does not usually occur as a result of excessive production of Aβ, but rather the ability of neurons to clear the peptide prior to aggregation is impaired (Mawuenyega et al., 2012). Our data demonstrates that the addition of SG1 to a solution of Aβ slows the aggregation of Aβ possibly allowing the body's natural clearance mechanisms to “catch up”. The slowing of aggregation may be sufficient for the physiological clearance of amyloid aggregates before they become pathological.

Previous methods used to test the effectiveness of amyloid inhibitors required several hours of preparation, followed by running an SDS-PAGE gel (Lee et al., 2012), or incubation (in the case of AFM imaging) (Gestwicki et al., 2004). In the case of single molecule AFS, a set of chemically modified cantilevers and substrates can be prepared in advance, and once the cantilever is loaded into the AFM two sets of experiments (control and inhibitor test) can be conducted within about 30 min. In this work we have shown a good correlation between experimental data obtained with force measurements (AFS), AFM imaging and molecular dynamics simulations, which demonstrated that the SG1 synthetic inhibitor disrupts the typical Aβ–Aβ nucleation pathway.

5. Conclusions

We conclude that synthetic inhibitor SG1 successfully disrupts the typical Aβ aggregation pathway by inhibiting binding of individual Aβ peptide molecules. Single molecule atomic force spectroscopy can be used to test compounds which act as specific competitive inhibitors for amyloid fibril formation. Notably, we were able to test the efficacy of SG1 inhibitor in only 30 min. This approach can potentially be used by the pharmaceutical industry as a high throughput screening technique to rapidly test various inhibitors for amyloid aggregation as well as a wide variety of other drug candidates which block the interaction of two molecules.

Acknowledgments

The authors wish to thank Westgrid and Compute Canada for generous use of computational resource for molecular dynamics simulations, and Professor Scott Taylor (University of Waterloo) and his laboratory for synthesis of APS. The authors acknowledge funding from Natural Science and Engineering Research Council (NSERC), Canada Foundation of Innovation (CFI) and Ontario Research Fund (ORF) grants to Z.L., NSERC grants to A.R., and NSERC Undergraduate Research Award to B.L.

References

Berendsen, H., van der Spoel, D., van Drunen, R., 1995. Comput. Phys. Commun. 91 (1–3), 43–56.
Bertram, L., Tanzi, R., 2005. J. Clin. Investig. 115 (6), 1449–1457.
Binnig, G., Quate, C., Gerber, C., 1986. Phys. Rev. B 56 (9), 930–933.
Bush, A., Tanzi, R., 2008. Neurotherapeutics 5 (3), 421–432.
Chiti, F., Dobson, C., 2009. Nat. Chem. Biol. 5 (1), 15–22.
Citron, M., 2004. Nat. Rev. Neurosci. 5 (9), 677–685.
DiPaolo, G., Kim, T., 2011. Nature 12 (5), 284–296.
Fezoui, Y., Hartley, D., Harper, J., Khurana, R., Walsh, D., Condron, M., Selkoe, D., Lansbury, P., Fink, A., Teplow, D., 2000. Int. J. Exp. Clin. Investig. 7 (3), 166–178.
Gestwicki, J., Crabtree, G., Graef, I., 2004. Science 306 (5697), 865–869.
Glabe, C., 2008. J. Biol. Chem. 283 (44), 29639–29644.
Hane, F., Tran, G., Attwood, S., Leonenko, Z., 2013. PLoS One 8, e59005.
Harper, J., Lansbury, P., 1997. Annu. Rev. Biochem. 66, 385–407.
Hess, B., Kutzner, C., van der Spoel, D., Lindahl, E., 2008. J. Chem. Theory Comput. 4 (3), 435–447.
Hinterdorfer, P., Dufrêne, Y., 2006. Nature 3 (5), 347–355.
Hutter, J., Bechhoefer, J., 1993. Rev. Sci. Instrum. 64 (7), 1868–1873.
Kim, B., Palermo, N., Lovas, S., Zaikova, T., Keana, J., Lyubchenko, Y., 2011. Biochem. J. 50 (23), 5154–5162.
Lambert, M., Barlow, A., Chromy, B., Edwards, C., Freed, R., Liosatos, M., Morgan, T., Rozovsky, I., Trommer, B., Viola, K., Wals, P., Zhang, C., Finch, C., Krafft, G., Klein, W., 1998. Proc. Natl. Acad. Sci. U.S.A. 95 (11), 6448–6453.
Lee, Y., Kim, H., Kim, Y., Seo, J., Roh, E., Han, H., Shin, K., 2012. Bioorg. Med. Chem. 20, 4921–4935.
Lindahl, E., Hess, B., van der Spoel, D., 2001. J. Mol. Model. 7, 306–317.
Mawuenyega, K., Sigurdson, W., Ovod, V., Munsell, L., Kasten, T., Morris, J., Yarasheski, K., Bateman, R., 2012. Science 330 (6012), 1774.
Mothana, B., Roy, S., Rauk, A., 2009. ARKIVOC v, pp. 116–134.
Neugroschl, J., Sano, M., 2010. Mt. Sinai J. Med. 77 (1), 3–16.
Petkova, A., Ishii, Y., Balbach, J., Antzutkin, O., Leapman, R., Delalio, F., Tycko, R., 2002. Proc. Natl. Acad. Sci. U.S.A. 99 (26), 16742–16747.
Roberson, E., Mucke, L., 2006. Science 314, 781–784.
Roy, S., 2010. Ph.D. Dissertation, University of Calgary.
Roy, S., Rauk, A., 2005. Med. Hypothesis 65 (1), 123–137.
Sciarretta, K., Gordon, D., Petkova, A., Tycko, R., Meredith, S., 2005. Biochemistry 44 (16), 6003–6014.
Stefani, M., 2012. Prog. Neurobiol. 99 (3), 226–245.
Tjernberg, L., Lilliehook, C., Callaway, D., Naslund, J., Hahne, S., Thyberg, J., Terenius, L., Nordstedt, C., 1997. J. Biol. Chem. 272 (19), 12601–12605.
Tjernberg, L., Naeslund, J., Lindqvist, F., Johansson, J., Karlstroem, A., Thyberg, J., Terenius, L., Nordstedt, C., 1996. J. Biol. Chem. 271 (15), 8545–8548.
Van der Spoel, D., Lindahl, E., Hess, B., Groenhof, G., Mark, A., Berendsen, H., 2005. J. Comput. Chem. 26 (16), 1701–1718.
Whitehouse, P., Martino, A., Antuono, P., Lowenstein, P., Coyle, J., Price, D., Kellar, K., 1986. Brain Res. 371 (1), 146–151.